Efficient GPS receiver DCB estimation for ionosphere modeling using satellite-receiver geometry changes

Chang-Ki Hong[1], Dorota A. Grejner-Brzezinska[2], and Jay Hyoun Kwon[1]

[1]*Department of Geoinformatics, The University of Seoul, Siripdae-gil 13, Dongdaemun-gu, Seoul 130-743, Korea*
[2]*Department of Civil and Environmental Engineering and Geodetic Science, The Ohio State University, Columbus, Ohio 43210, USA*

(Received June 25, 2008; Revised October 27, 2008; Accepted November 4, 2008; Online published November 13, 2008)

A new and efficient algorithm using the geometry conditions between satellite and tracking receivers is proposed to determine the receiver differential code bias (DCB) using permanent reference stations. This method does not require a traditional single-layer ionosphere model and can be used for estimating DCBs of receivers in a regional network as long as one of the receiver DCBs is already known. The main underlying rationale for this algorithm is that the magnitude of the signal delay caused by the ionosphere is, under normal conditions, highly dependent on the geometric range between the satellite and the receiver. The proposed algorithm was tested with the Ohio Continuously Operating Reference Stations (CORS) sub-network data. The results show that quality comparable to the traditional DCB estimation method is obtainable by implementing this simple algorithm.
Key words: GPS, receiver DCB, ionosphere modeling, CORS.

1. Introduction

The geometry-free linear combination is frequently used for the recovery of total electron content (TEC) from the GPS observations because all of the geometry-related terms, such as the ranges between satellites and receivers, the tropospheric effect, and the satellite and receiver clock errors, can be eliminated. The only remaining terms, after the geometry-free linear combination is formed from the phase-smoothed code observation, are the ionospheric delay, differential code biases (DCBs) in the GPS satellites and the receivers, and the measurement noises (Schaer, 1999). As the magnitude of the combined satellite and receiver DCBs can reach up to several nanoseconds (ns), DCBs in both the satellite and receiver are known to be the main errors in the estimation of TEC using GPS (Sardon and Zarraoa, 1997). According to Wilson and Mannucci (1994), the TEC, when estimated from GPS measurements, may result in ± 3 ns and ± 10 ns errors, respectively, when either the satellite or receiver DCB is ignored. Therefore, it can be said that the estimation of DCBs is a crucial part of ionosphere modeling using GPS. In general, DCBs are estimated together with the single layer ionosphere model. This procedure requires a thin-shell model assumption and, as a consequence, a mapping function to convert slant TEC to vertical TEC (Sardon *et al*., 1994; Komjathy, 1997; Schaer, 1999; Otsuka *et al*., 2002). This mapping function depends on the selected altitude of the single layer and plays a key role in the separation of the ionospheric delay from the receiver DCBs in the observation equation. Thus, the estimated DCBs are highly dependent on the selected ionosphere model. To overcome this limitation, a new and efficient approach to determine the receiver DCBs using a geometric condition between the satellite and receivers is proposed. The proposed method is more computationally efficient than the existing techniques, and its use eliminates the requirement for a model of the ionosphere.

2. Methodology

2.1 Single-difference GPS observations

As the noise level of the P-code GPS measurements is relatively high, the phase-smoothed P-code (SC) GPS observations are frequently used for ionosphere modeling (Schaer, 1999; Otsuka *et al*., 2002; Wielgosz *et al*., 2003). One of the more useful linear combinations used to remove the common errors, such as tropospheric delay, satellite and receiver clock errors, relativistic effect in GPS data processing, is the so-called geometry-free linear combination. This linear combination is formed by subtracting $\tilde{P}^k_{i,2}$ from $\tilde{P}^k_{i,1}$, as shown in Eq. (1) (Schaer, 1999; Wielgosz *et al*., 2003).

$$E\left\{\tilde{P}^k_i\right\} = E\left\{\tilde{P}^k_{i,1} - \tilde{P}^k_{i,2}\right\} = F \cdot I^k_i + \Delta b^k + \Delta b_i, \qquad F := \left(1 - f_1^2/f_2^2\right) \tag{1}$$

where $E\{\cdot\}$ is the expectation operator; subscript i and superscript k represent the indices of the receiver and the satellite, respectively; $\tilde{P}^k_i$ is the geometry-free SC (GSC) observation; $\tilde{P}^k_{i,1}$ and $\tilde{P}^k_{i,2}$ are SC observations on L1 and L2, respectively; $f_1 (= 1575.42\,\text{MHz})$ and $f_2 (= 1227.60\,\text{MHz})$ are carrier frequencies; I^k_i is ionospheric delay on $\tilde{P}^k_{i,1}$; Δb^k and Δb_i are the differential, inter-frequency hardware delays of the receiver and satellite, respectively (generally called DCBs).

The single-difference (SD) GSC is obtained by distinguishing between two simultaneous observations of satellite k, tracked by two stations, i and j. The satellite-dependent

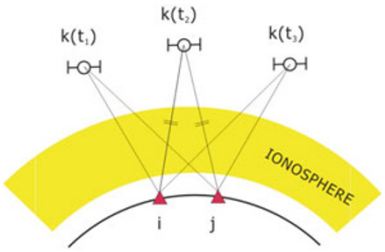

Fig. 1. SD geometric-range changes with respect to time.

error, i.e., satellite DCB, is then cancelled out, and the corresponding formula is shown in Eq. (2), as follows:

$$E\left\{\tilde{P}_{ij}^{k}\right\} = E\left\{\tilde{P}_{i}^{k} - \tilde{P}_{j}^{k}\right\} = F \cdot I_{ij}^{k} + \Delta b_{ij}, \qquad \Delta b_{ij} := \Delta b_{i} - \Delta b_{j}, \quad I_{ij}^{k} := I_{i}^{k} - I_{j}^{k} \tag{2}$$

where, $\tilde{P}_{ij}^{k}$ is the SD GSC measurement, I_{ij}^{k} is SD ionospheric delay.

As can be observed in Eq. (2), the SD GSC observations depend on the SD ionospheric delay scaled by F, and a bias (constant term).

2.2 SD geometric ranges and ionospheric delay changes

The main idea for the determination of the receiver DCB in this study is that SD GSC observations are inevitably affected by the SD geometry; this means that the observations are subject to both variations in the ionosphere and changes in the geometric-range between the satellite and the tracking stations. Figure 1 illustrates the changes in the satellite-receiver geometry with respect to time (t_1, t_2, t_3), in particular the SD geometric range changes.

As can be seen in Fig. 1, the SD ionospheric delays vary with respect to time because of the varying length of the signal path within the ionospheric layer. Therefore, it can be expected that the SD ionospheric delay change significantly depends on the SD geometric range, which in turn represents a dominant part of the SD observations. Namely, the effect of geometry change determines the overall trend of the SD ionospheric delay, and the remaining local ionospheric disturbance represents a "residual variation" with respect to time. Hence, it is expected that the dominant part of the SD ionospheric delay is zero when the computed SD geometric range equals zero (at epoch t_2 in Fig. 1). This property of the SD approach directly supports the determination of the SD receiver DCBs, Δb_{ij}, from Eq. (2). Also, it should be mentioned that the assumption that the local ionospheric variations can be neglected for a short data span is made in this approach. The procedure is discussed in more detail in the following section.

2.3 Estimation of the SD receiver DCB

The first step in the estimation of the SD receiver DCBs is the selection of baselines over the entire GPS network because, in principle, SD receiver DCB is determined on a baseline basis. The next step is the selection of a continuous data span from the SD GSC that satisfies the following conditions (for one satellite per baseline):

- The computed SD geometric range curve has a zero value at a specific epoch within the continuous data span.
- The correlation coefficient between the SD GSC, and SD geometric range curve is greater than the predefined empirical value (>0.7).

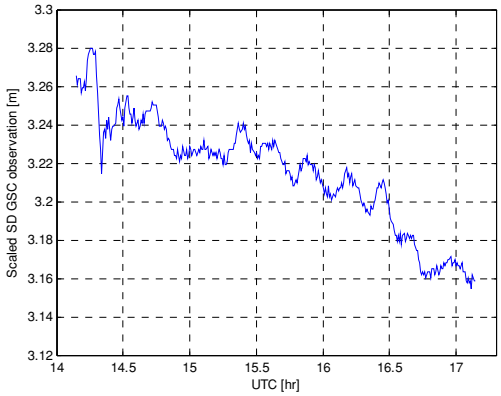

Fig. 2. Variations in the scaled SD GSC observations with respect to time (PRN:4, baseline:TIFF-KNTN).

The critical value for the correlation coefficient is determined by analyzing the computed correlation coefficients between continuous SD GSCs and corresponding SD geometric-range curves. More details on this are described in Section 4.

To show that the observations are directly dependent on the SD ionospheric delays, Eq. (2) is divided by the scale factor, F. The scaled SD GSC measurements then show the variations caused by the actual SD ionospheric delay variations because the scaled SD receiver DCB is constant over a period of at least 1 day (Sardon *et al.*, 1994; Sardon and Zarraoa, 1997).

Figure 2 shows an example of a continuous span of the scaled SD GSC observations, $\tilde{P}_{ij}^{k}/F$. The SD ionospheric delay variations have, in this example, a decreasing trend with small fluctuations. Figure 3 shows the corresponding SD geometric-range curve in meters; it is expected that the SD ionospheric delays and the SD geometric ranges follow a similar trend. The computed correlation coefficient between the scaled SD GSC observations (Fig. 2) and the SD geometric-range curve (Fig. 3) is 0.9.

The SD ionospheric delays can be determined from SD GSC using the geometry between the GPS satellite and the two stations, since we assume that the SD geometric range is the major factor that dominates the overall trend of the SD observations. The geometric ranges are computed using the precise orbit ephemerides as published by the International GNSS Service (IGS), and the known station coordinates. Finally, one can find continuous data spans which contain the epoch for which SD geometric range is zero and then determine the SD receiver DCB between the two stations.

As mentioned earlier, SD ionospheric delays, I_{ij}^{k}, generally follow the trend of the SD geometric range, R_{ij}^{k}, so that the linear relation between them can be introduced as follows:

$$I_{ij}^{k}(t) = \alpha \cdot R_{ij}^{k}(t) + \beta \tag{3}$$

where, α is scale factor, and β is constant term.

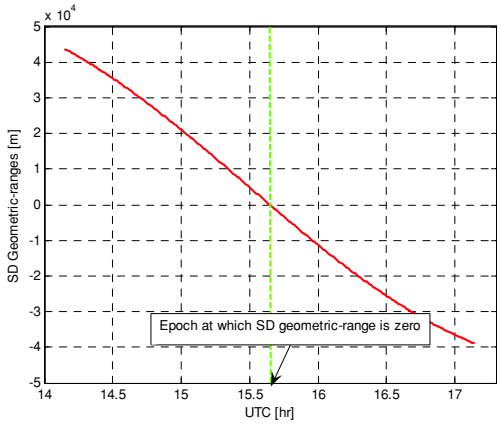

Fig. 3. SD geometric-range curve (PRN:4, baseline:TIFF-KNTN).

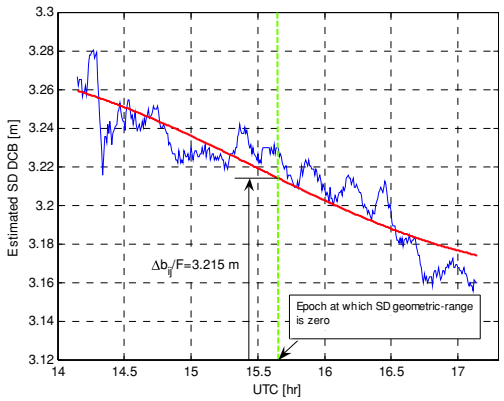

Fig. 4. An example of estimated SD DCB (PRN:4, baseline:TIFF-KNTN).

Then, Eq. (2) can be rewritten as

$$E\left\{\tilde{P}_{ij}^{k}(t)\right\} = F\left[\alpha \cdot R_{ij}^{k}(t) + \beta\right] + \Delta b_{ij}. \tag{4}$$

As can be seen in Eq. (4), the parameter Δb_{ij} cannot be separated from β because both terms are linear offsets. However, if an epoch at which the SD geometric range is zero within a continuous data span can be found, then a condition, such that the SD ionospheric delay is zero at epoch t_o (i.e., at epoch t_2 in Fig. 1), can be introduced.

$$I_{ij}^{k}(t_o) = 0, \quad R_{ij}^{k}(t_o) = 0 \Rightarrow \beta = 0 \tag{5}$$

Thus, Eq. (4) can be simplified, as shown in Eq. (6), for the estimation of the SD receiver DCBs. It should be noted that Eq. (6) is valid only when t_o exists for a continuous data span.

$$E\left\{\tilde{P}_{ij}^{k}(t)\right\} = \begin{bmatrix} F \cdot R_{ij}^{k}(t) & 1 \end{bmatrix} \begin{bmatrix} \alpha \\ \Delta b_{ij} \end{bmatrix} \tag{6}$$

where α and Δb_{ij} are the parameters to be estimated.

Figure 4 presents an example of an SD DCB estimated using the data shown in Figs. 2 and 3. The red line corresponds to the computed values from the estimated parameters, i.e., $\alpha \cdot R_{ij}^{k}(t) + \Delta b_{ij}/F$. Once the SD receiver DCBs are obtained for the network, this information is used to recover the undifference (UD) DCBs by fixing one receiver's DCB with the known value, as shown in Eq. (7), if it is available from an external source.

$$E\left\{\begin{bmatrix} \Delta\bar{b}_{ij} \\ \Delta\bar{b}_{i} \end{bmatrix}\right\} = \begin{bmatrix} 1 & -1 \\ 1 & 0 \end{bmatrix} \begin{bmatrix} \Delta b_i \\ \Delta b_j \end{bmatrix} \tag{7}$$

where $\Delta\bar{b}_i$ is the fixed receiver DCB, and $\Delta\bar{b}_{ij}$ is the estimated SD receiver DCB between the stations i and j.

3. Numerical Results

The proposed method for the estimation of receiver DCBs can be applied to a local or regional GPS network. To demonstrate the performance of the proposed algorithm, we selected 14 geometrically well-distributed continuously operating reference stations (CORS), with a separation of approximately 80 km between stations, within the state of Ohio network. To analyze the consistency of the estimated receiver DCBs, we used the data from three consecutive days (01–03 April 2004; day of year (DOY) 92–94). Figure 5 shows the locations of the Ohio CORS and selected baselines for the determination of the SD receiver DCBs. The baselines with lengths less than 200 km were selected among all possible station pairs (39 in this case) for the sufficient redundancy in solving the system (Eq. (7)).

Once the baselines for the whole network are selected, the SD GSC observables for each baseline can be obtained from the GPS measurements. The corresponding SD geometric ranges can also be computed using the precise ephemerides information published by IGS and known station coordinates published by the National Geodetic Survey (NGS) (http://www.ngs.noaa.gov).

To analyze the correlation between SD GSC and SD geometric range, the correlation coefficient between them is computed. Figure 6 illustrates the number of continuous data spans—SD GSC data with no cycle slips—with respect to the computed correlation coefficients for the three consecutive days. As seen in Fig. 6, in general, the SD GSC depends significantly on the SD geometric ranges. The negative or low correlation coefficients may occur when the effect of local ionospheric disturbance is dominant in the SD GSC. Therefore, the correlation coefficient of 0.7 is selected as a cutoff to improve the reliability of the solutions.

The next step is to find the satellites that satisfy the required conditions, as explained in Section 2.3. This pro-

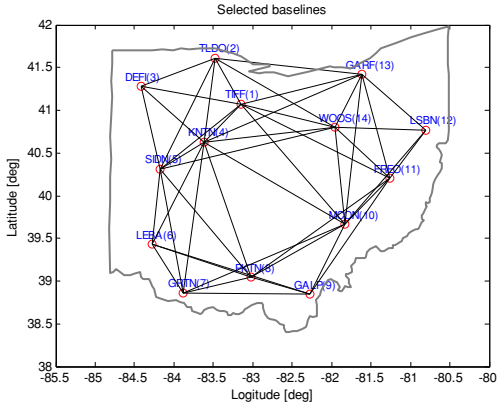

Fig. 5. Selected baselines for the determination of SD receiver DCBs (Ohio CORS network).

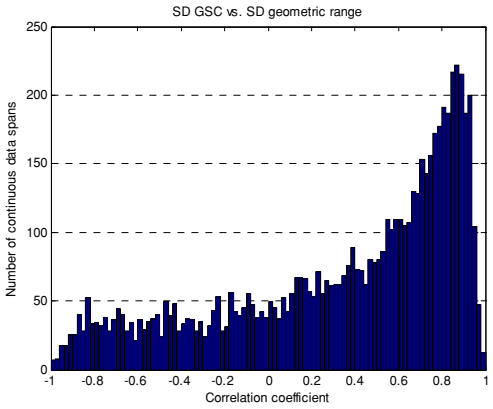

Fig. 6. Histogram of correlation coefficients between the SD GSC and SD geometric-range curve; three days of data were used.

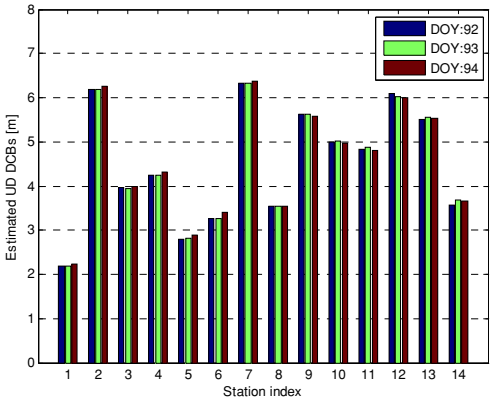

Fig. 7. Estimated UD receiver DCBs using the proposed method.

cedure should be repeated for all selected baselines. During a day, each baseline may observe one or more satellites that meet the required condition and can be used for the determination of the SD receiver DCBs. Once the SD receiver DCBs, Δb_{ij}, are obtained for each baseline, the UD receiver DCBs for all the stations are computed using the least-squares method by fixing one of the receiver DCB, as shown in Eq. (7). The UD receiver DCB of the TIFF station obtained from the BERNESE software, i.e., the reference value, is used as a datum constraint, and the total number of SD receiver DCBs to compute UD receiver DCBs are 68, 93, 63 for DOY92, DOY93, DOY94, respectively. Figure 7 presents the estimated UD receiver DCBs obtained from the proposed method for the three consecutive days showing excellent consistencies.

The true reference values for the receiver DCBs are not available at this time. Hence, the estimated receiver DCBs for DOY92, DOY93, and DOY94 are compared with the corresponding daily solution from BERNESE software (Hugentobler *et al.*, 2001) by processing the same datasets. Figure 8 shows the differences between the reference and the estimated UD receiver DCBs. The maximum difference is less than 15 cm, which corresponds to 3.3% of the average DCB magnitude. This clearly confirms that the proposed method generates the comparable results. Notice that the reference UD receiver DCBs of FREO and LSBN on DOY 94 are not available since BERNESE software did not

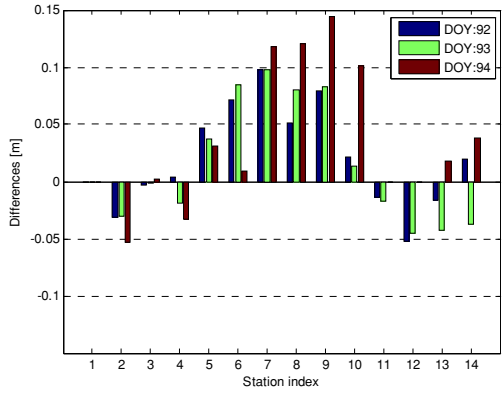

Fig. 8. Differences between the reference and the estimated UD receiver DCBs.

generate the solution giving notice of bad data quality.

4. Summary and Conclusions

A new and efficient method to determine the receiver DCB is proposed and its applicability demonstrated using a reference GPS network. The principle rationale of the proposed method is that ionospheric delays in GPS measurements are inherently affected by the actual geometric range between satellite and receiver. Consequently, receiver UD DCBs can be estimated using SD measurements if one of receiver DCBs is already known. The proposed algorithm was applied to the Ohio CORS network, and the results showed that the mean differences between the estimated receiver DCBs using the proposed method and reference values were 4 cm. Thus, the quality of the UD receiver DCBs estimated using the proposed method was comparable to the reference values, i.e., solutions from the BERNESE software. We also demonstrated that the proposed method was stable for three consecutive days.

References

Hugentobler, U., S. Schaer, and P. Fridez, *BERNESE GPS Software Version 4.2*, 537 pp., Astronomical Institute, University of Berne, 2001.

Komjathy, A., Global ionospheric total electron content mapping using the global positioning system, Technical report No. 188, Department of Geodesy and Geomatics Engineering, University of New Brunswick, 1997.

Otsuka, Y., T. Ogawa, A. Saito, T. Tsugawa, S. Fukao, and S. Miyazaki, A new technique for mapping of total electron content using GPS network in Japan, *Earth Planets Space*, **54**, 63–70, 2002.

Sardon, E. and N. Zarraoa, Estimation of total electron content using GPS data: How stable are the differential satellite and receiver instrumental biases?, *Radio Sci.*, **32**(5), 1899–1910, 1997.

Sardon, E., A. Ruis, and N. Zarraoa, Estimation of the transmitter and receiver differential biases and the ionospheric total electron content from Global Positioning System observations, *Radio Sci.*, **29**(3), 577–586, 1994.

Schaer, S., Mapping and Predicting the Earth's Ionosphere Using the Global Positioning System, Ph.D. Thesis, Astronomical Institute, University of Berne, Switzerland, 1999.

Wielgosz, P., D. Grejner-Brzezinska, I. Kashani, and Y. Yi, Instantaneous Regional Ionosphere Modeling, *Proceedings of ION GPS/GNSS 2003*, 1750–1757, 2003.

Wilson, B. and A. Mannucci, Extracting ionospheric measurements from GPS in the presence of Anti-Spoofing, *Proceedings of ION GPS-94*, 1599–1608, 1994.

C.-K. Hong (e-mail: ckhong@uos.ac.kr), D. A. Grejner-Brzezinska, and J. H. Kwon